The RAG Recombinase Dictates Functional Heterogeneity and Cellular Fitness in Natural Killer Cells

Jenny M. Karo,[1] David G. Schatz,[2] and Joseph C. Sun[1,*]
[1]Immunology Program and Gerstner Sloan Kettering Graduate School of Biomedical Sciences, Memorial Sloan Kettering Cancer Center, New York, NY 10065, USA
[2]Department of Immunobiology and the Howard Hughes Medical Institute, Yale University School of Medicine, New Haven, CT 06510, USA
*Correspondence: sunj@mskcc.org
http://dx.doi.org/10.1016/j.cell.2014.08.026

SUMMARY

The emergence of recombination-activating genes (RAGs) in jawed vertebrates endowed adaptive immune cells with the ability to assemble a diverse set of antigen receptor genes. In contrast, innate lymphocytes, such as natural killer (NK) cells, are not believed to require RAGs. Here, we report that NK cells unable to express RAGs or RAG endonuclease activity during ontogeny exhibit a cell-intrinsic hyperresponsiveness but a diminished capacity to survive following virus-driven proliferation, a reduced expression of DNA damage response mediators, and defects in the repair of DNA breaks. Evidence for this novel function of RAG has also been observed in T cells and innate lymphoid cells (ILCs), revealing an unexpected role for RAG proteins beyond V(D)J recombination. We propose that DNA cleavage events mediated by RAG endow developing adaptive and innate lymphocytes with a cellular "fitness" that safeguards their persistence later in life during episodes of rapid proliferation or cellular stress.

INTRODUCTION

The recombination-activating gene proteins RAG1 and RAG2 (collectively, RAG) mediate V(D)J gene rearrangement at the antigen receptor loci during lymphocyte development, giving rise to lymphocytes with unique specificity and providing the molecular mechanism behind Burnet's theory of clonal selection. In contrast to T and B cells, natural killer (NK) cells classically represent a third lineage of lymphocytes that possess germline-encoded antigen receptors and do not require receptor gene rearrangement for their development (Kondo et al., 1997). Given that NK cells do not require V(D)J recombination or express surface immunoglobulin (Ig) or T cell receptor (TCR) proteins, they are not thought to require RAG proteins for their development, function, or survival. Indeed, NK cells are present in normal numbers in RAG-deficient mice, whereas T and B cells are completely absent (Mombaerts et al., 1992; Shinkai et al., 1992). There is as yet no evidence that RAG plays a physiological role in any cell type other than B and T lymphocytes or in any process other than V(D)J recombination.

Although NK cells have long been classified as a component of the innate immune system, recent evidence suggests that this cell type possesses traits attributable to adaptive immunity (Sun and Lanier, 2011). These characteristics include "education" mechanisms to ensure self-tolerance during NK cell development and clonal-like expansion of antigen-specific NK cells during viral infection, followed by the ability to generate long-lived "memory" NK cells. However, the underlying molecular mechanisms that control NK cell function and longevity, resulting in distinct effector and memory NK cell subsets during pathogen challenge, are not known. Furthermore, it is unknown whether functional heterogeneity or discrete cell subsets exist within effector and memory NK cell populations or their naïve precursors, as has been observed in responding CD8^{+} T cells (Kaech and Wherry, 2007).

V(D)J recombination is an intricate and tightly regulated process for generating lymphocyte receptor diversity and is initiated by the binding of the RAG complex to target recombination signal sequences (RSSs) at the antigen receptor loci to generate DNA double-strand breaks (DSBs) (Helmink and Sleckman, 2012). RAG1 contains the endonuclease catalytic center (Fugmann et al., 2000b; Kim et al., 1999; Landree et al., 1999), which is active in the presence of its binding partner, RAG2 (Oettinger et al., 1990). RAG2 also contributes a plant homeodomain finger that targets the complex to activated or "open" chromatin through binding of histone 3 trimethylated at lysine 4 (H3K4me3) (Ji et al., 2010; Liu et al., 2007; Matthews et al., 2007). Following cleavage, the broken DNA ends are stabilized in a postcleavage complex by RAG (Agrawal and Schatz, 1997; Hiom and Gellert, 1998) and ataxia telangiectasia-mutated (ATM) kinase (Bredemeyer et al., 2006; Helmink and Sleckman, 2012), and shuttled into the nonhomologous end-joining (NHEJ) pathway for DNA repair (Gellert, 2002; Lee et al., 2004). The introduction of DSBs activates several phosphoinositide 3-kinase-like Ser/Thr kinases, including DNA-dependent protein kinase (DNA-PK) and ATM, which orchestrate the DNA damage response (Nussenzweig and Nussenzweig, 2010). High fidelity is required in this system because aberrant rearrangement events can lead to genomic

instability and lymphoid malignancies (Lieber et al., 2006; Mills et al., 2003). Interestingly, mice deficient in various members of the V(D)J recombination and NHEJ machinery demonstrate varying degrees of T and B cell deficiencies but generally possess an intact, albeit largely uncharacterized, NK cell population.

Numerous studies have linked RAG to DNA breaks and chromosomal rearrangements (including translocations) at "cryptic" RSSs and non-RSS sequences outside of antigen receptor loci (Gostissa et al., 2011; Lieber et al., 2006; Mills et al., 2003; Papaemmanuil et al., 2014). Furthermore, RAG2 has been shown to bind to thousands of sites of active chromatin in the lymphocyte nucleus (Ji et al., 2010), providing a plausible mechanism by which RAG nuclease activity could be delivered to many locations in the genome. However, although the genome-wide activity of RAG has been strongly linked to pathological consequences, it has not been suggested previously to play a beneficial role in cellular development or function.

Although the generation of the lymphoid compartment has been studied extensively, unifying models of lymphocyte development have been difficult to construct, and the ontogeny of NK cells is not well understood. Mice that report RAG expression or a history of RAG expression ("fate-mapping" mice) have revealed that a large number of mouse common lymphoid progenitors (CLPs) that are destined to become B cells or commit to the NK cell lineage express RAG (Borghesi et al., 2004; Welner et al., 2009). As expected, all mature B cells exhibit a history of RAG expression. However, a surprisingly large fraction of NK cells (~40%) have also been shown to derive from RAG-expressing CLPs. In support of this, independent studies have shown that NK cells can possess nonproductive rearrangements within their Ig and TCR loci (Borghesi et al., 2004; Fronková et al., 2005; Lanier et al., 1992; Pilbeam et al., 2008). The physiological relevance of RAG expression during NK cell ontogeny has remained unexplored.

Here we use RAG fate-mapping and RAG-deficient mice to demonstrate that selective RAG expression during NK cell ontogeny gives rise to functionally heterogeneous populations of effector cells within the peripheral NK cell pool. We demonstrate that RAG-deficient NK cells are more prone to apoptosis at a steady state, contain a greater amount of phosphorylated histone H2AX (γ-H2AX) indicative of genomic instability, and are less efficient at processing or repairing genomic breaks during DNA damage. RAG-deficient NK cells had reduced levels of DNA damage response mediators such as DNA-dependent protein kinase catalytic subunit (DNA-PKcs), Ku80, and ATM, and these repair enzymes have also been shown to be critical for cell survival following virus infection. These findings identify a surprising and novel role for RAG in the functional specialization of NK cells that involves conferring cellular fitness in NK cell subsets via endonuclease activity and mechanisms beyond V(D)J recombination.

RESULTS

Selective RAG Expression during Ontogeny Distinguishes Functional Heterogeneity within the NK Cell Population

Using RAG fate-mapping mice (Rag1^{Cre} x Rosa26-floxed STOP-tdRFP) (Welner et al., 2009), we observed that 40%–50% of bone

marrow NK cells and 20%–30% of peripheral NK cells have at one point expressed RAG1 (i.e., are marked by red fluorescent protein [RFP] expression) (Figure 1A), consistent with previous findings (Borghesi et al., 2004; Ichii et al., 2010; Lanier et al., 1992; Pilbeam et al., 2008). Analysis of the NK lineage in RAG2^{YFP} knockin reporter mice (Igarashi et al., 2001; Kuwata et al., 1999) revealed the highest levels of RAG expression in CLPs from bone marrow, with expression decreasing as NK cells undergo maturation (Figure 1B). Interestingly, NK cells that lack evidence of prior RAG expression during development (RFP⁻) were more activated and terminally differentiated (i.e., higher KLRG1 expression) in all organs (Figure 1C) and demonstrated a higher degree of cytotoxicity (Figure 1D) compared with NK cells that expressed RAG (RFP⁺). Given that peripheral NK cells do not express RAG (as determined by RAG2^{YFP} reporter mice, Figure 1E), our data demonstrate that selective RAG expression during NK cell ontogeny correlates with functionally distinct progeny cells and heterogeneity in the peripheral NK cell pool.

RAG Deficiency Results in NK Cells with a Cell-Intrinsic Hyperresponsiveness

We next investigated whether NK cells lacking Rag were phenotypically and functionally similar to RFP⁻ NK cells in fate-mapping mice. Mice deficient in Rag2 lack peripheral T and B cells (Shinkai et al., 1992), but contain normal NK cell numbers compared with wild-type (WT) mice (Figure S1 available online). Nevertheless, Rag2$^{-/-}$ NK cells exhibited a more mature (KLRG1^{hi}, CD27^{lo}, CD11b^{hi}) and activated (CD69^{hi}, CD62L^{lo}) phenotype at steady state compared with WT NK cells (Figures 2A and 2B), consistent with a previous report (Andrews and Smyth, 2010). Furthermore, similar to RFP⁻ NK cells in fate-mapping mice, Rag2$^{-/-}$ NK cells were more cytotoxic on a per cell basis in vitro and in vivo compared with WT NK cells (Figures 2C and 2D). A similar hyperresponsiveness was observed in Rag2$^{-/-}$ NK cells in mixed bone marrow chimeric mice where lethally irradiated WT mice were injected with equal numbers of WT (CD45.1) and Rag2$^{-/-}$ (CD45.2) bone marrow cells and allowed to reconstitute the hematopoietic compartment (Figure 2E). We noted that the phenotype of Rag2$^{-/-}$ NK cells in the mixed chimera setting was not as pronounced as in NK cells isolated directly from Rag2$^{-/-}$ mice, suggesting that both intrinsic and extrinsic factors might contribute to NK cell hyperresponsiveness in nonirradiated Rag2$^{-/-}$ mice. Similar observations were made in NK cells from Rag1$^{-/-}$ mice (Figure S2).

RAG-Deficient NK Cells Fail to Expand and Persist following MCMV Infection

To investigate whether RAG influences other NK cell functions, we used a well established viral model of antigen-specific NK cell expansion (Sun et al., 2009). In this model, NK cells expressing the mouse cytomegalovirus (MCMV)-specific activating receptor Ly49H undergo robust antigen-driven proliferation (100- to 1000-fold expansion) following MCMV infection, and following viral clearance, a population of long-lived memory NK cells persists in both lymphoid and nonlymphoid organs (Sun et al., 2009). When equal numbers of splenic WT (CD45.1) and Rag2$^{-/-}$ (CD45.2) Ly49H-expressing NK cells were adoptively cotransferred into Ly49H-deficient mice, followed by infection
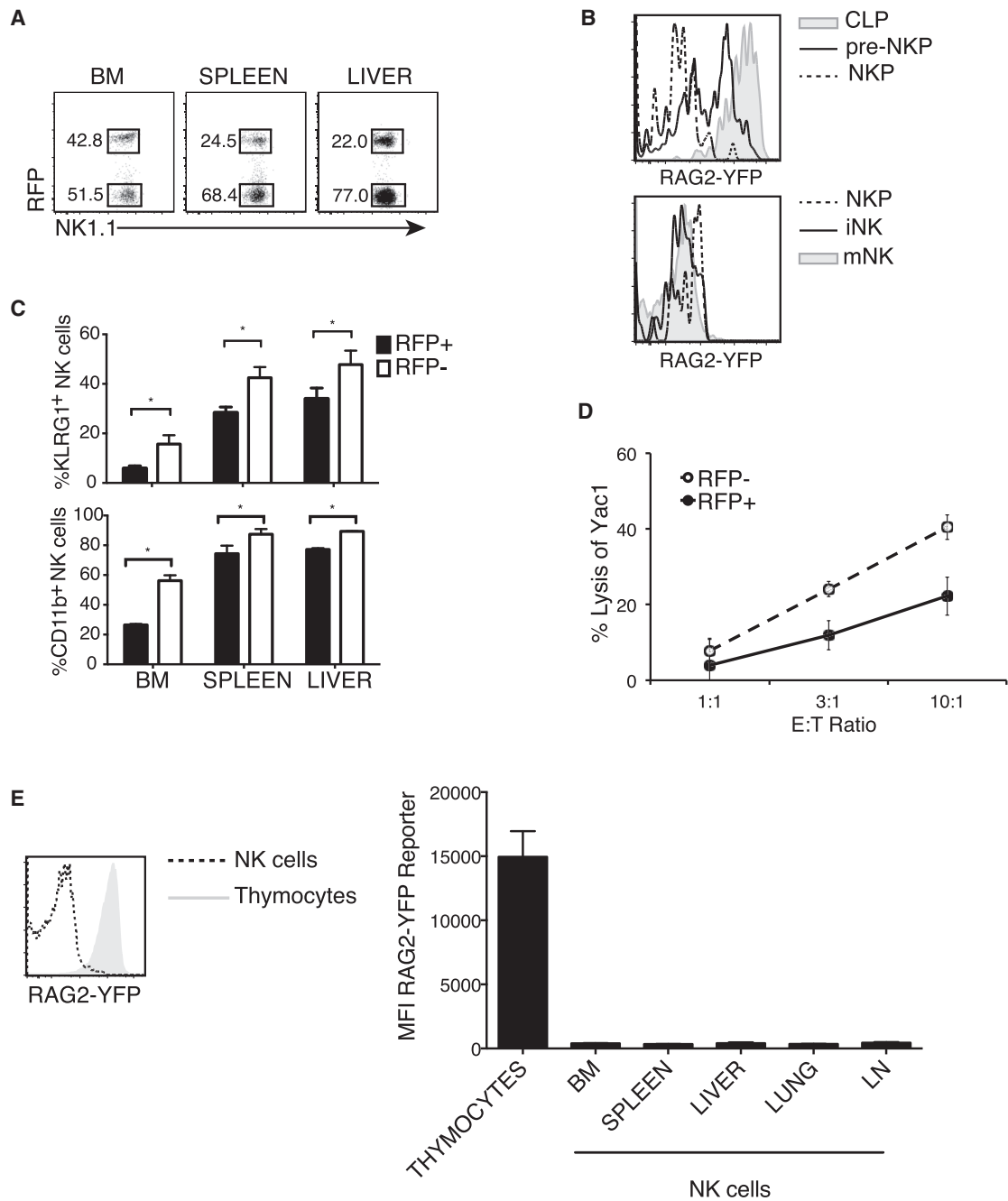
Figure 1. History of RAG Expression Delineates Heterogeneity within the NK Cell Population

(A) NK1.1$^+$ TCRβ$^-$ NK cells from various organs of $Rag1^{Cre}$ x $ROSA^{TdRFP}$ mice were analyzed for RFP expression. BM, bone marrow.

(B) Flow cytometric analysis of YFP expression was performed on bone marrow of $Rag2^{YFP}$ mice using FLT3 and CD122 to identify CLP (FLT3$^+$ CD122$^-$), pre-NK cell progenitor (NKP) (FLT3$^-$ CD122$^-$), and NKP (FLT3$^-$ CD122$^+$) within the lineage-negative (Lin$^-$) CD27$^+$ CD127$^+$ cell population (top flow plot), and NK1.1 and DX5 were used to identify NKP (NK1.1$^-$DX5$^-$), immature NK cells (iNK) (NK1.1$^+$ DX5$^-$), and mature NK cells (mNK) (NK1.1$^+$ DX5$^+$) cells within the Lin$^-$ CD122$^+$ population (bottom flow plot). Lin$^-$ is defined as CD19$^-$ CD3$^-$ TCRβ$^-$ CD4$^-$ CD8$^-$ Ter119$^-$.

(C) NK1.1$^+$ TCRβ$^-$ NK cells from various organs of $Rag1^{Cre}$ x $ROSA^{TdRFP}$ mice were analyzed for activation and maturation markers (KLRG1 and CD11b). Error bars for all graphs show SEM, and all data are representative of n = 3-4 mice in three independent experiments. *p < 0.01.

(D) Percent lysis of ^{51}Cr-labeled Yac1 target cells by sorted RFP$^+$ (solid line) and RFP$^-$ (dashed line) NK cells ex vivo. Data are representative of three independent experiments performed with n = 3–5 mice. E:T, effector:target.

(E) NK1.1$^+$ TCRβ$^-$ NK cells from various organs of RAG2-YFP reporter mice were analyzed for YFP expression at steady state and compared with TCRβ$^+$ thymocytes. Quantification and a representative histogram are shown. The results shown are representative of three independent experiments (n = 3-4 mice). LN, lymph node.
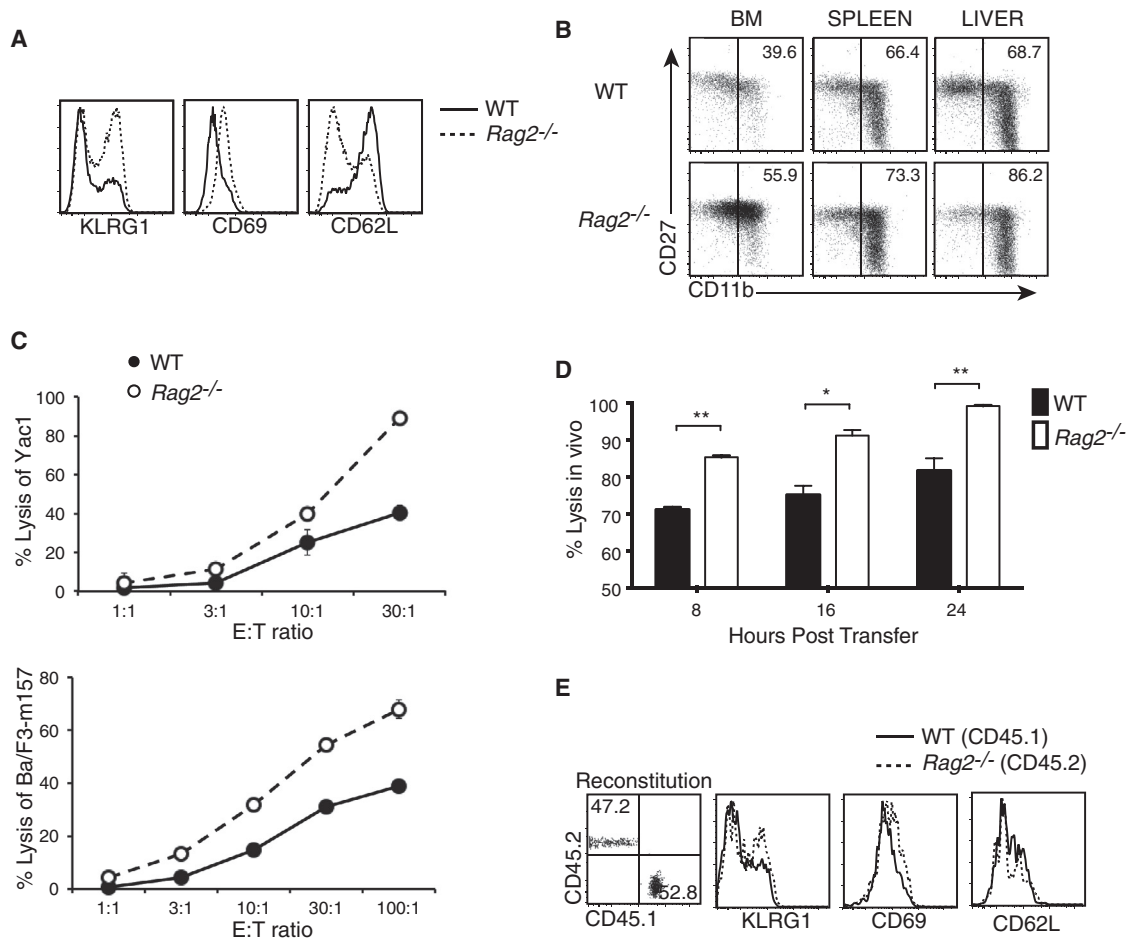
Figure 2. Lack of RAG Produces a Cell-Intrinsic Hyperresponsiveness in NK Cells

(A and B) Splenic NK cells from WT and Rag2-deficient ($Rag2^{-/-}$) mice were analyzed for the activation and maturation markers KLRG1, CD69, and CD62L (A) and CD27 and CD11b (B).

(C) Percent lysis of ^{51}Cr-labeled Yac1 and Ba/F3-m157 target cells by WT and $Rag2^{-/-}$ NK cells ex vivo. Data are representative of three independent experiments performed with n = 3–5 mice.

(D) Percentage of CFSE-labeled β2m-deficient target cells lysed by NK cells in vivo in WT and $Rag2^{-/-}$ mice at the indicated time points after transfer. Error bars show SEM, and the data depict three to five mice per group, repeated in three independent experiments. *p < 0.05, **p < 0.005.

(E) Lethally irradiated mice were injected with equal numbers of WT (CD45.1) and $Rag2^{-/-}$ (CD45.2) bone marrow cells. Following hematopoietic reconstitution, NK cells were analyzed for the activation markers shown.

See also Figure S2.

with MCMV (Figure 3A), the WT NK cells expanded more robustly than $Rag2^{-/-}$ NK cells in the first 7 days postinfection (PI), and continued to persist at a greater percentage for over a month (Figures 3B–3D). The defect in $Rag2^{-/-}$ NK cell expansion during MCMV infection was observed in all organs (Figure 3E), demonstrating that diminished $Rag2^{-/-}$ NK cell numbers in the peripheral blood were not due to aberrant trafficking or retention in nonlymphoid tissues. Donor NK cells from $Rag1^{-/-}$ mice were similarly outcompeted by WT NK cells following adoptive transfer and MCMV infection (Figures 3F and 3G) in both lymphoid and nonlymphoid organs (Figure 3H).

WT NK cells outcompeted RAG-deficient NK cells following MCMV infection, regardless of whether the donor NK cells were derived directly from individual WT and $Rag2^{-/-}$ mice (Figures 3B–3D), or from WT:$Rag2^{-/-}$ or WT:$Rag1^{-/-}$ mixed bone marrow chimeric mice (i.e., a T and B cell replete environment, Figures 4A and 4B). In contrast, NK cells from athymic nude, TCRβ-deficient, major histocompatibility complex class II-deficient, or activation-induced cytidine deaminase (AID)-deficient mice behaved like WT NK cells (Figure S3 and data not shown), further underscoring that development in the absence of T cells or AID activity could not solely account for the defect of NK cells from Rag-deficient mice. Adoptive transfer of NK cells from WT:$Rag2^{-/-}$ mixed bone marrow chimeric mice into $Rag2^{-/-}$ x $Il2rg^{-/-}$ hosts (which lack B, T, and NK cells) also demonstrated that $Rag2^{-/-}$ NK cells were compromised compared with WT NK cells (Figure 4C). This rules out the possibility that reduced recovery of $Rag2^{-/-}$ NK cells is simply due to their being selectively rejected in the Ly49H-deficient hosts. Additionally, we performed an "add back" experiment in which young $Rag2^{-/-}$ mice
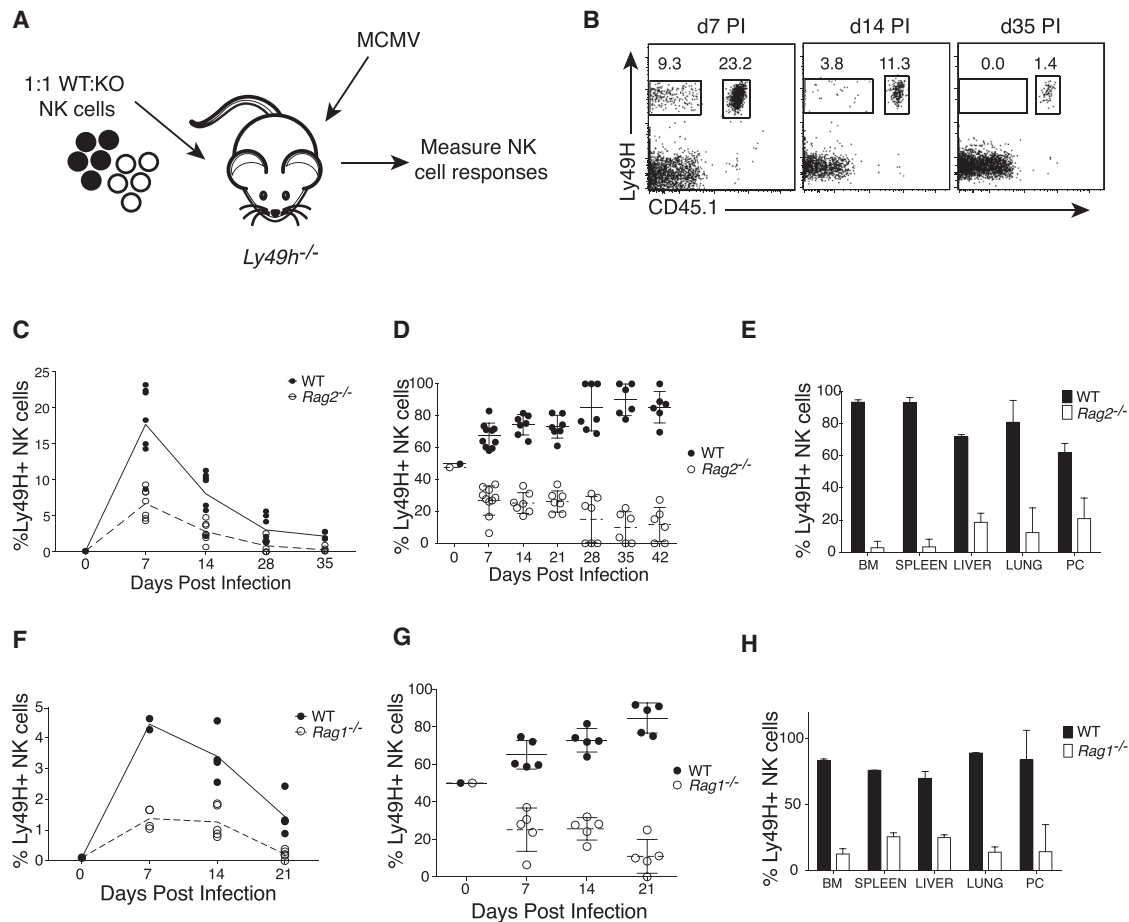
Figure 3. Rag-Deficient NK Cells Fail to Expand following MCMV Infection

(A) Schematic of the experiment. Equal numbers of WT (CD45.1) and *Rag2*$^{-/-}$ (CD45.2) Ly49H$^+$ NK cells were cotransferred into Ly49H-deficient (*Ly49h*$^{-/-}$) mice prior to infection with MCMV. KO, knockout.

(B–D) Representative flow cytometric plots of adoptively transferred WT versus *Rag2*$^{-/-}$ Ly49H$^+$ NK cells in peripheral blood at various time points following MCMV infection (B). Graphs depict the absolute (C) and relative (D) percentages of each experimental group, and data are representative of five independent experiments (n = 5–10 mice per time point), with each data point representing an individual mouse. d, day.

(E) The percentage of transferred WT and *Rag2*$^{-/-}$ Ly49H$^+$ NK cells in the indicated organs at day 10 PI. Error bars show SEM, and the graph is representative of three independent experiments with four to five mice per group. PC, peritoneal cavity.

(F and G) Equal numbers of WT and *Rag1*$^{-/-}$ Ly49H$^+$ NK cells were cotransferred into *Ly49h*$^{-/-}$ mice, and, following MCMV infection, the absolute (F) and relative (G) percentages of adoptively transferred populations in peripheral blood are shown for various time points. Data are representative of three independent experiments (n = 3–5 mice per time point).

(H) The percentage of transferred WT and *Rag1*$^{-/-}$ Ly49H$^+$ NK cells in the indicated organs at day 10 PI. Error bars show SEM, and the graph is representative of three independent experiments with four to five mice per group.

were given T and B cells to reconstitute the lymphopenic compartment. After 8 weeks, *Rag2*$^{-/-}$ NK cells from add back mice were still unable to expand as robustly as WT NK cells following MCMV infection (Figure 4D). Finally, we sorted RFP$^+$ and RFP$^-$ NK cells from RAG fate-mapping mice and observed that RFP$^+$ cells outcompeted RFP$^-$ cells following MCMV infection when NK cell populations were normalized prior to adoptive cotransfer (Figure 4E). Because neither the mixed bone marrow chimeric setting nor the add back environment were able to rescue the proliferation and survival of *Rag2*$^{-/-}$ NK cells during viral infection, we conclude that RAG deficiency leads to a cell-intrinsic defect in NK cells. Moreover, we confirmed that mature NK cells do not re-express *Rag* during viral infection

(using *RAG*^{YFP} reporter mice; Figure 4F), consistent with the interpretation that RAG activity during NK cell ontogeny initiates a program of enhanced cellular fitness that influences the peripheral response of mature NK cells to viral infection.

Impaired Survival of RAG-Deficient NK Cells

We next investigated whether the impaired expansion of *Rag2*$^{-/-}$ NK cells during MCMV infection was due to diminished proliferation or impaired survival. When WT and *Rag2*$^{-/-}$ NK cells were labeled with carboxyfluorescein succinimidyl ester (CFSE) prior to adoptive transfer and viral infection, similar rates and numbers of cell division were observed on days 3 and 5 PI (Figure S4), indicating that *Rag2*$^{-/-}$ NK cells can proliferate
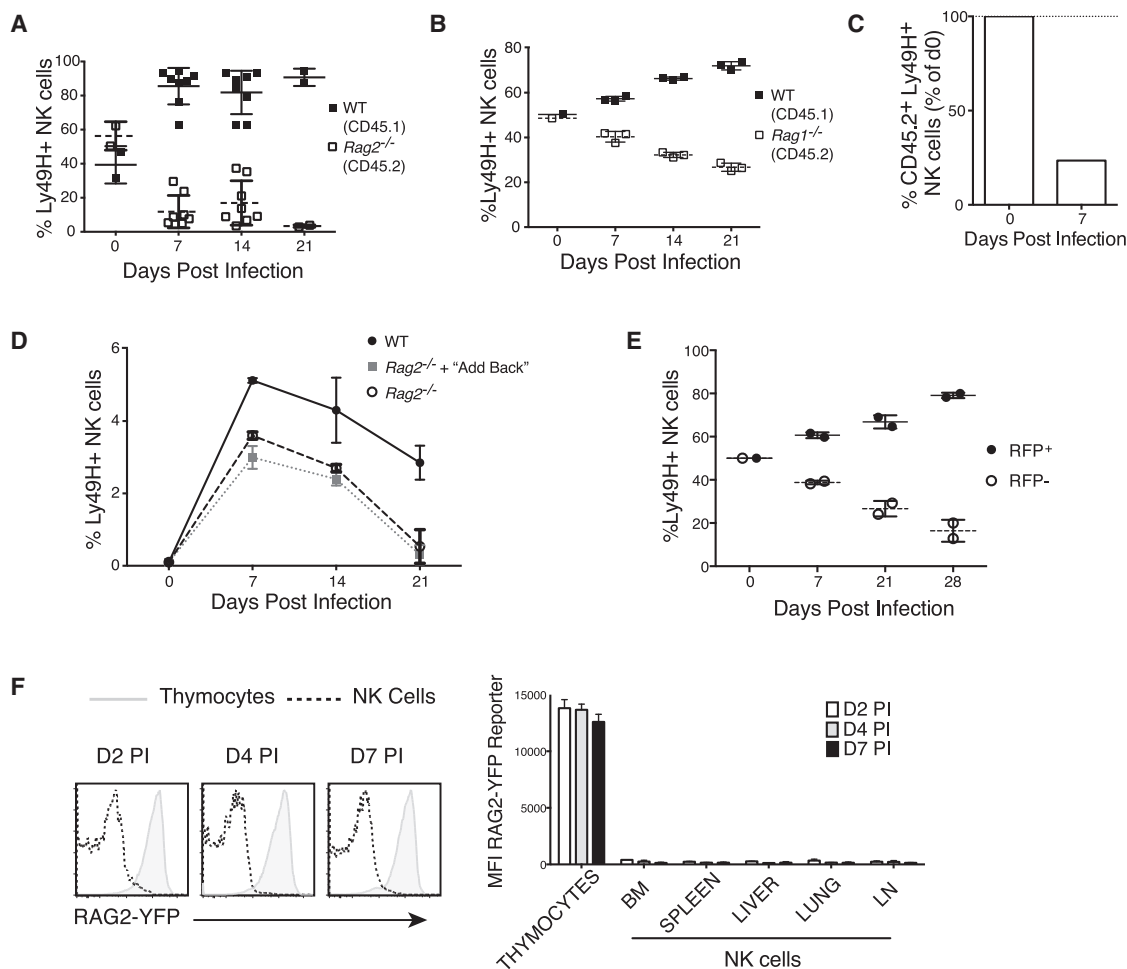
Figure 4. Inability of RAG-Deficient NK Cells to Expand and Persist following MCMV Infection Is Cell Intrinsic

(A) Splenic Ly49H$^+$ NK cells from mixed WT:$Rag2^{-/-}$ bone marrow chimeric mice were adoptively transferred, and percentages of donor populations are shown at various time points after MCMV infection. Data are representative of three independent experiments each (with three to seven mice per time point).

(B) As in (A), but using WT:$Rag1^{-/-}$ bone marrow chimeric mice.

(C) Splenic Ly49H$^+$ NK cells from mixed WT:$Rag2^{-/-}$ bone marrow chimeric mice were adoptively transferred into $Rag2^{-/-}xIl2rg^{-/-}$ hosts, and, following MCMV infection, donor NK cell populations were analyzed at day 7 PI.

(D) Splenic T and B cells were transferred and parked for 8-12 weeks to reconstitute the lymphopenic compartment of young $Rag2^{-/-}$ mice ("Add Back" mice). Ly49H$^+$ NK cells from "Add Back", WT, and $Rag2^{-/-}$ mice were adoptively transferred, and NK cell percentages in the peripheral blood at various time points following MCMV infection are shown. Results are representative of three independent experiments (n = 3–5 mice).

(E) RFP$^+$ and RFP$^-$ NK cells were sorted from RAG fate-mapping mice and equal numbers adoptively cotransferred into $Ly49h^{-/-}$ mice. Percentages of donor populations are shown at various time points after MCMV infection. Data are representative of two independent experiments (with two mice per time point).

(F) NK cells from various organs of $Rag2^{YFP}$ reporter mice were analyzed for YFP expression at days 2, 4, and 7 after MCMV infection and compared with thymocytes. Quantification and representative histograms are shown. Error bars show SEM, and results are representative of three independent experiments (n = 3–5 mice).

normally in response to viral challenge. In contrast, $Rag2^{-/-}$ NK cells were significantly more susceptible to apoptosis at steady state and following MCMV infection, as demonstrated by the significantly higher population staining positive for fluorescent labeled inhibitor of caspases (FLICA), a membrane-permeable probe retained in cells containing active caspases (Figure 5A and data not shown). Furthermore, when NK cells from WT:$Rag2^{-/-}$ chimeric mice were pulsed with 5-bromo-2′-deoxyuridine (BrdU) and chased to examine the rate of decay of labeled cells, the BrdU-labeled $Rag2^{-/-}$ NK cells declined

more rapidly in number than WT NK cells (Figure 5B). Together, these findings suggest that RAG expression during NK cell development potentiates the optimal survival of peripheral NK cells.

RAG-Deficient NK Cells Contain More DNA Double-Strand Breaks and Reduced Levels of DNA Repair Enzymes

To investigate why $Rag2^{-/-}$ NK cells are more prone to apoptosis, even at steady state, we assessed the levels of
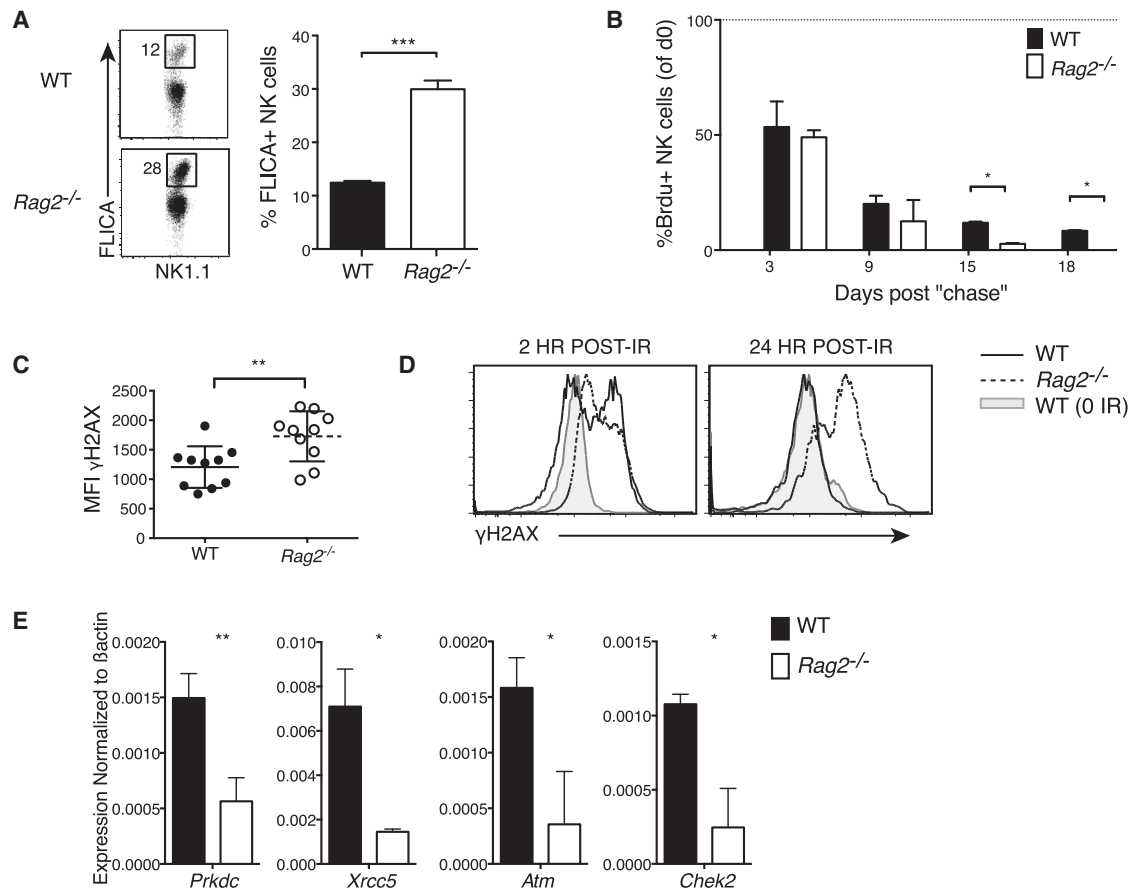
Figure 5. RAG Deficiency during Ontogeny Produces NK Cells with Greater Genomic Instability Because of Reduced DNA Break Repair

(A) Representative plots and graph show FLICA staining (for pan-caspase activation) in splenic Ly49H^{+} NK cells from uninfected mice. Error bars show SEM, and data are representative of three independent experiments (n = 3–5 mice). *p < 0.05, ***p < 0.0005.

(B) $Rag2^{-/-}$:WT mixed bone marrow chimeras were pulsed with BrdU (0.8 mg/ml) drinking water, and the decrease in percent BrdU^{+} NK cells at days after chase with normal water was determined. Day 0 marks when mice stopped receiving BrdU water and started to receive normal water. Error bars show SEM, and data are representative of three independent experiments (n = 3–5 mice). *p < 0.05.

(C) Mean fluorescence intensity (MFI) of γ-H2AX on splenic NK cells from WT and $Rag2^{-/-}$ mice. Data are representative of three independent experiments (n = 5–10 mice), with each data point representing an individual mouse. **p < 0.005.

(D) WT and $Rag2^{-/-}$ NK cells from mixed bone marrow chimeric mice were irradiated (IR, 10 Gy), and the phosphorylation of H2AX was analyzed by flow cytometry at various time points post-IR. Representative histograms show irradiated WT (solid) and $Rag2^{-/-}$ (dashed) NK cells compared with nonirradiated cells (0 IR, gray).

(E) $Prkdc$, $Xrcc5$, Atm, and $Chek2$ mRNA levels were quantified by qRT-PCR in sorted WT and $Rag2^{-/-}$ NK cells. Gene expression levels are normalized to β-actin. The results shown are representative of three independent experiments. *p < 0.05, **p < 0.005.

See also Table S1.

phosphorylated γ-H2AX in WT and $Rag2^{-/-}$ NK cells as a measure of DNA DSBs and global genomic instability (Fernandez-Capetillo et al., 2004; Rogakou et al., 1998, 2000). Notably, $Rag2^{-/-}$ NK cells showed higher levels of γ-H2AX compared with WT NK cells by flow cytometry (Figure 5C). In eukaryotic cells, small amounts of ionizing radiation (IR) induce DNA DSBs and γ-H2AX focus formation (Rogakou et al., 1998), followed by DNA DSB repair and subsequent removal of the γ-H2AX mark. Therefore, to compare the DSB repair response of WT and $Rag2^{-/-}$ NK cells, we measured γ-H2AX levels at various time points after exposure to low levels of radiation (10 Gy). As expected, WT NK cells upregulated γ-H2AX within 2 hr of radiation treatment, followed by clearance of γ-H2AX

foci within 24 hr (Figure 5D). In contrast, $Rag2^{-/-}$ NK cells showed a delay in upregulation of γ-H2AX and a marked defect in their ability to clear γ-H2AX foci, indicating a defect in processing or repair of DSBs (Figure 5D, dashed line). These findings suggest that NK cells lacking RAG activity during ontogeny both accumulate evidence of DNA damage at steady state and have difficulty mediating a DNA repair response following the acute introduction of DNA damage.

Because RAG functions to generate DNA DSBs during V(D)J recombination in developing T and B cells (Chen et al., 2000; Helmink and Sleckman, 2012), it seemed counterintuitive that RAG deficiency would result in elevated levels of basal DSBs in resting NK cells. However, one important consequence of

RAG-mediated DSBs in lymphocytes is the activation of DNA repair and the induction of a broad program of changes in gene expression that includes factors involved in the DNA damage response (Bredemeyer et al., 2008; Helmink and Sleckman, 2012). Therefore, we hypothesized that loss of RAG in developing NK cells could result in diminished expression or activity of DNA damage repair enzymes and, therefore, contribute to genomic instability when DSBs arise as a result of proliferation or cellular stress. In support of this hypothesis, $Rag2^{-/-}$ NK cells have been found to have lower transcript levels of DNA-dependent protein kinase catalytic subunit (DNA-PKcs), ATM, Ku80 (Xrcc5), and Chek2 (an essential protein downstream of ATM; Helmink and Sleckman, 2012) compared with WT NK cells (Figure 5E). Because ATM and DNA-PKcs have serine/threonine kinase activity and are thought to phosphorylate H2AX (Chen et al., 2000; Fernandez-Capetillo et al., 2004; Helmink and Sleckman, 2012; Rogakou et al., 1998), a decrease in their levels might explain the delay in upregulation of γ-H2AX in irradiated $Rag2^{-/-}$ NK cells. Decreased levels of DNA-PKcs and Ku80 may also explain the higher rate of apoptosis in $Rag2^{-/-}$ NK cells compared with WT NK cells (Figure 5A) because both DNA-PKcs and Ku80 are critical for NHEJ (Bredemeyer et al., 2008; Helmink and Sleckman, 2012), and reduced levels could reduce DSB repair and maintenance of DNA integrity.

Diminished Cellular Fitness in Hyperresponsive NK Cells from SCID Mice

Our data indicate that RAG deficiency results in diminished DNA-PKcs in NK cells. To ascertain whether these diminished DNA-PKcs levels might fully or partially account for the survival defect of $Rag2^{-/-}$ NK cells during viral infection, we analyzed NK cells from severe combined immunodeficiency (SCID) mice, which harbor a naturally occurring nonsense mutation in DNA-PKcs (Blunt et al., 1996; Bosma et al., 1983; Fulop and Phillips, 1990). Although DNA-PKcs is required for V(D)J recombination and, therefore, T and B cell development, SCID animals are similar to RAG-deficient animals in that they harbor normal NK cell numbers (Figure S5A). Indeed, like RAG-deficient NK cells, we found that NK cells from SCID mice exhibited an activated phenotype (Figure 6A) and increased cytotoxic potential (Figure 6B) but diminished survival following MCMV infection compared with WT NK cells (Figure 6C). SCID NK cells could not be recovered in any organs by 3 weeks PI, in contrast to the robust generation of long-lived NK cells from WT mice (Figure 6D). In addition, SCID NK cells had higher γ-H2AX levels compared with WT NK cells (Figure 6E) but were delayed in γ-H2AX upregulation and clearance following IR treatment (Figure S5B). Because our result in mice with the spontaneous SCID mutation mirrors the findings in $Rag1$- and $Rag2$-deficient mice, this alleviates potential complications and unwanted phenotypes from genetic knockout mice generated by incorporation of a neomycin selection marker. Taken together, our data support a model where RAG is required for optimal DNA-PKcs expression in NK cells and in which DNA-PKcs, in turn, has an important role in maintaining lymphocyte genomic stability and survival following DNA damage, as occurs during rapid proliferation.

Defective Response of NK Cells Expressing Catalytically Inactive RAG

To determine whether the NK cell phenotype observed in RAG-deficient mice is due to the absence of RAG protein per se or the absence of RAG-mediated DNA cleavage, we analyzed active-site RAG1 mutant mice on a $Rag1$-deficient background ($Rag1^{-/-}$ D708A) (Ji et al., 2010). The D708A mutant RAG1 protein expressed by these bacterial artificial chromosome transgenic mice lacks DNA cleavage activity but interacts with RAG2 and binds DNA normally (Fugmann et al., 2000a; Ji et al., 2010; Kim et al., 1999; Landree et al., 1999). Similar to $Rag1^{-/-}$ and $Rag2^{-/-}$ NK cells, NK cells from $Rag1^{-/-}$ D708A mice exhibited an activated and terminally differentiated phenotype at steady state and in mixed bone marrow chimeras (Figure 6F and data not shown). During MCMV infection, $Rag1^{-/-}$ D708A NK cells also exhibited impaired effector cell numbers compared with WT NK cells (Figure 6G). Like $Rag1^{-/-}$ NK cells, $Rag1^{-/-}$ D708A NK cells contained higher levels of γ-H2AX at steady state compared with WT NK cells (Figure 6H). Therefore, expression of catalytically inactive RAG1 does not rescue the defective expansion, suggesting that RAG-mediated DNA cleavage during ontogeny is required for complete cellular fitness of NK cells responding to viral infection.

RAG Expression in Adaptive and Innate Lymphocytes Confers Cellular Fitness

To investigate the consequence of RAG-mediated genomic stability in other lymphocyte populations during ontogeny, we compared TCR transgenic CD8^{+} T cells from OT-1 (RAG-competent) versus OT-1 x $Rag2^{-/-}$ mice (Hogquist et al., 1994). Although the OT-1 TCR is expressed early during thymocyte development in these mice, the RAG promoter is still active in the RAG-competent transgenic background (using RAG[GFP] reporter mice; P.J. Fink, personal communication). Therefore, the OT-1 system provides an opportunity to investigate T cell fitness in the presence or absence of RAG expression beyond its role in gene rearrangement at the antigen receptor loci. As with WT NK cells, CD8^{+} T cells from OT-1 mice upregulated γ-H2AX within 2 hr of radiation treatment, followed by clearance of γ-H2AX foci within 24 hr (Figure 7A). In contrast, CD8^{+} T cells from OTI-1 x $Rag2^{-/-}$ mice showed a delay in upregulation of γ-H2AX and a marked defect in their ability to clear γ-H2AX foci, indicating an inability to repair DSBs (Figure 7A, dashed line). Furthermore, similar to $Rag2^{-/-}$ NK cells, CD8^{+} T cells from OT-1 x $Rag2^{-/-}$ mice possessed lower transcript levels of DNA-PKcs, Ku80, and ATM compared with RAG-sufficient OT-1 CD8^{+} T cells (Figure 7B). Together, these findings suggest that NK and T lymphocytes that lack RAG activity during ontogeny are predisposed to genomic instability because of decreased levels of essential DNA damage repair proteins.

To determine whether RAG expression confers fitness in T cells, we transferred equal numbers of OT-1 and OT-1 x $Rag2^{-/-}$ CD8^{+} T cells into B6 mice and determined survival following infection with a recombinant MCMV expressing ovalbumin (Ova). We found that OT-1 x $Rag2^{-/-}$ cells possessed a reduced capacity for survival compared with OT-1 cells (Figure 7C), similar to our observations in NK cells. Furthermore, in vitro-cultured OT-1 and OT-1 x $Rag2^{-/-}$ CD8^{+} T cells
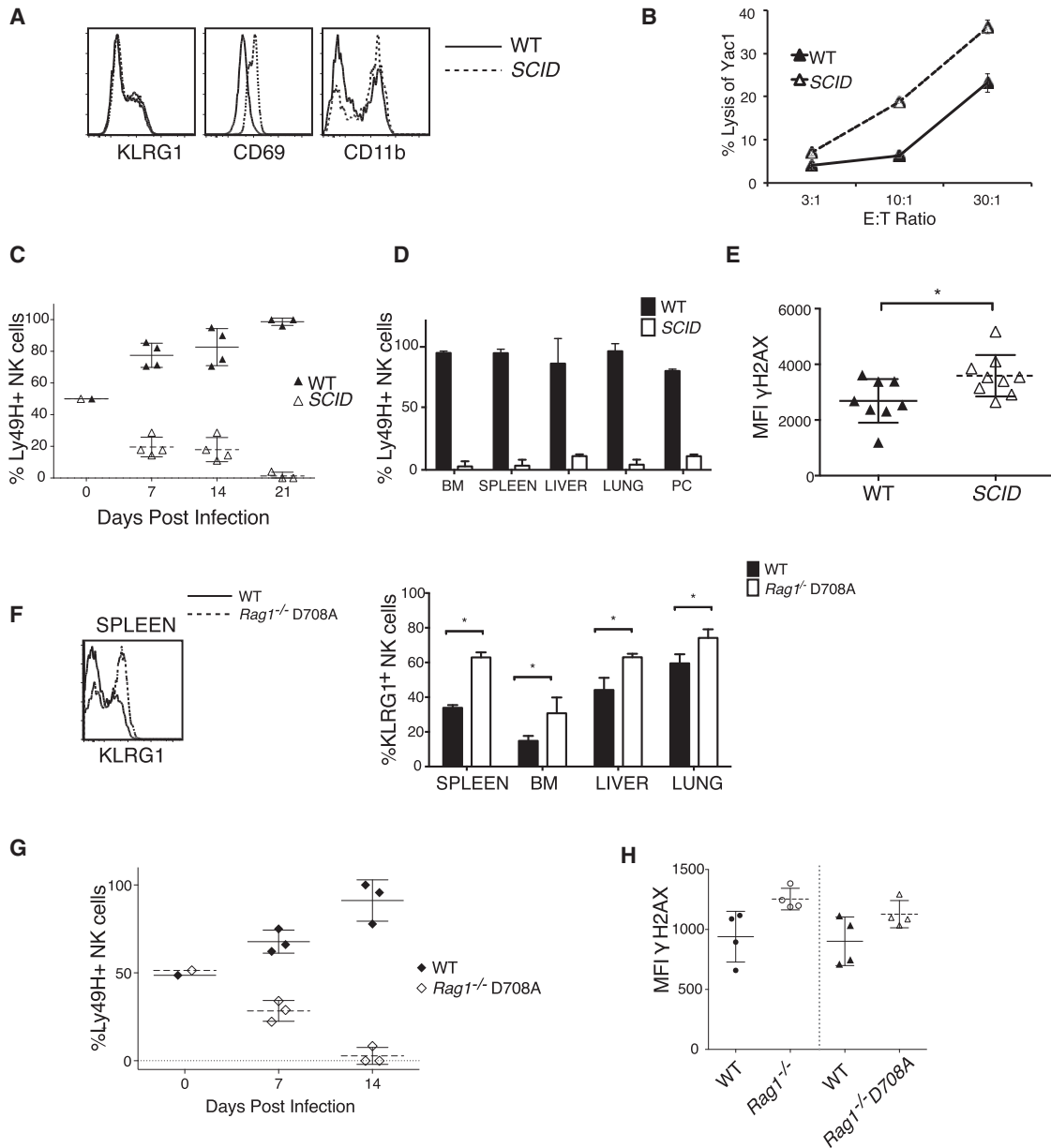
Figure 6. Diminished Cellular Fitness in Hyperresponsive NK Cells from SCID and *Rag1*^{−/−} D708A Mice

(A) Histograms showing expression of activation markers on WT and SCID NK cells.

(B) Percent lysis of ^{51}Cr-labeled Ba/F3-m157 (top) and Yac1 (bottom) target cells by WT and SCID NK cells ex vivo.

(C) Equal numbers of WT (CD45.1) and SCID (CD45.2) Ly49H$^+$ NK cells were cotransferred into *Ly49h*^{−/−} mice, and, following MCMV infection, the relative percentages of adoptively transferred populations in peripheral blood are shown for various time points. The results shown are representative of three independent experiments (n = 3–5 mice), with each data point representing an individual mouse.

(D) The percentage of transferred WT and SCID Ly49H$^+$ NK cells in the indicated organs at day 21 PI. Error bars show SEM, and data are representative of three independent experiments (n = 3-4 mice).

(E) MFI of γ-H2AX on splenic NK cells from WT and SCID mice. Data are representative of three independent experiments (n = 5–8 mice). *p < 0.05.

(F) NK cells from various organs of WT (CD45.1) and *Rag1*^{−/−} D708A (CD45.2) bone marrow chimeric mice were analyzed for the activation and maturation markers shown. Error bars show SEM, and data are representative of three independent experiments (n = 3–5 mice). *p < 0.05.

(G) Ly49H$^+$ NK cells from WT (CD45.1) and *Rag1*^{−/−} D708A (CD45.2) mixed bone marrow chimeric mice were cotransferred into *Ly49h*^{−/−} mice, and, following MCMV infection, the relative percentages of adoptively transferred populations in peripheral blood are shown for various time points. Results shown are representative of three independent experiments (n = 3–5 mice).

(H) MFI of γ-H2AX on splenic NK cells from WT:*Rag1*^{−/−} (circles) and WT:*Rag1*^{−/−} D708A (diamonds) bone marrow chimeric mice. Results are representative of three independent experiments (n = 4–5 mice). See also Figure S5.
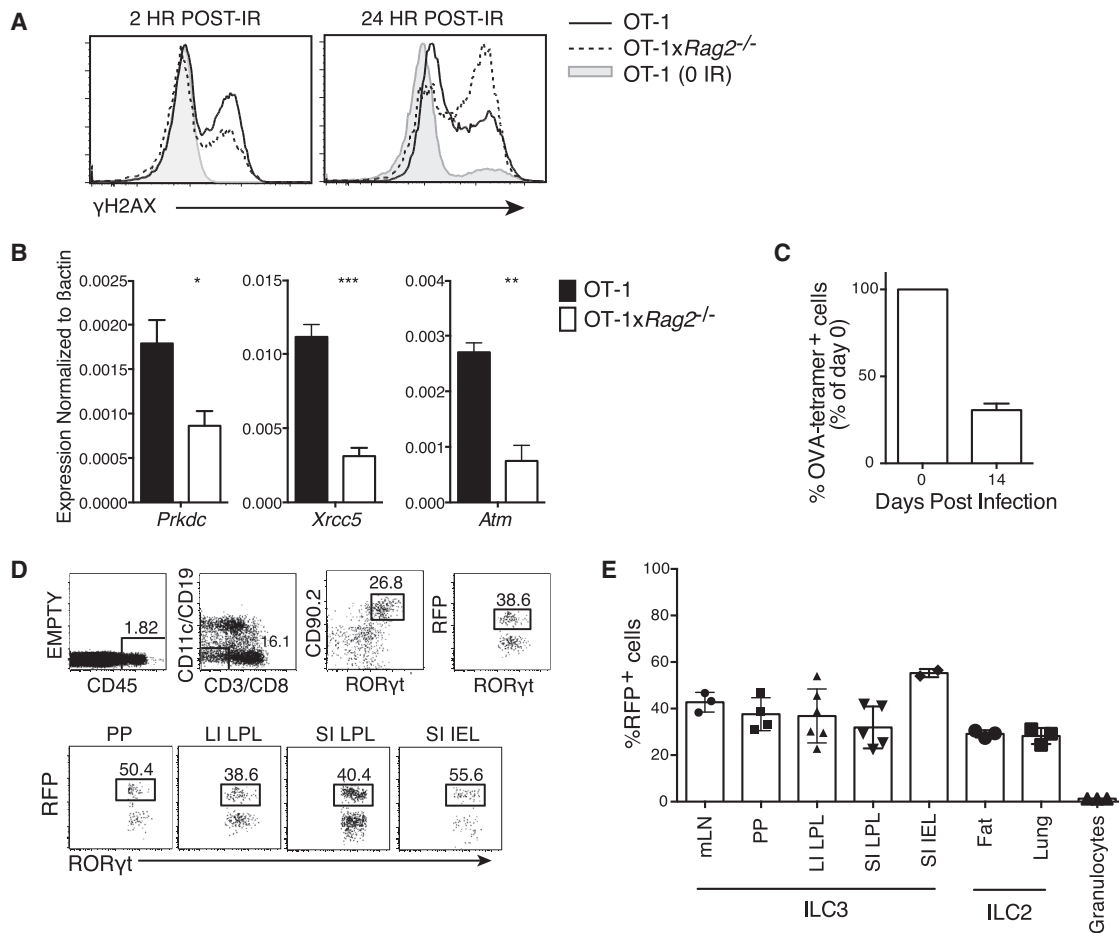
Figure 7. A Novel Role for RAG in the Cellular Fitness of Adaptive and Innate Lymphocytes

(A) CD8^{+} T cells from OT-1 and OT-1 x $Rag2^{-/-}$ mice were irradiated (10 Gy), and the phosphorylation of H2AX was analyzed by flow cytometry at various time points post-IR. Representative histograms show irradiated OT-1 (solid) and OT-1 x $Rag2^{-/-}$ (dashed) CD8^{+} T cells compared with nonirradiated cells (0 IR, gray).

(B) $Prkdc$, $Xrcc5$, and Atm mRNA levels were quantified by qRT-PCR in sorted CD8^{+} T cells from OT-1 and OT-1 x $Rag2^{-/-}$ mice. Gene expression levels are normalized to β-actin. The results shown are representative of three independent experiments. *p < 0.05, **p < 0.005, ***p < 0.0005.

(C) Equal numbers of CD8^{+} T cells from OT-1 (CD45.1x2) and OT-1 x $Rag2^{-/-}$ (CD45.1) mice were adoptively cotransferred into B6 mice (CD45.2), and the relative percentage of OT-1 x $Rag2^{-/-}$ cells to OT-1 cells was determined following MCMV-Ova infection.

(D and E) Group 2 and 3 innate lymphoid cells (ILC2 and ILC3) were isolated from various organs of RAG fate-mapping mice, and the percentage of RFP^{+} cells was determined by flow cytometry. The gating strategy for intestinal ILC3 (D) and quantified percentages of ILC3 and ILC2 in the indicated tissues is shown (E). See also Figures S6 and S7 and Table S1.

stimulated with Ova peptide (SIINFEKL) or anti-CD3/CD28 beads yielded a similar result (Figures S6A and S6B), demonstrating that RAG expression during ontogeny endows peripheral T cells with enhanced cellular fitness.

Innate lymphoid cells (ILCs) have recently been described to maintain tissue homeostasis and provide protection against pathogens at mucosal surfaces (e.g., gut, lung, and adipose tissue). Although the common γ chain cytokine receptor and cytokine IL-7 are required for ILC development, it is thought that RAG proteins are not essential (Spits and Cupedo, 2012). Here we examined group 2 and 3 ILCs in our RAG fate-mapping mice and observed that 30%–50% of these cells had a history of RAG expression during ontogeny (Figures 7D and 7E), consistent with a previous report on ILC2s (Yang et al., 2011). In addition, ILCs from $Rag2^{-/-}$ mice possessed higher γ-H2AX levels at

steady state compared with WT mice (Figure S7). Whether there is a functional consequence of the RAG-based heterogeneity in ILC populations at mucosal barriers is currently being investigated.

DISCUSSION

RAG proteins function during lymphocyte development to mediate V(D)J gene rearrangement at the antigen receptor loci, providing the adaptive immune system with a mechanism for assembling and diversifying its antigen receptor gene repertoire. Using RAG fate mapping and RAG-deficient mice, we were able to distinguish mature lymphocytes that have developed in the presence or absence of RAG expression and recombination and analyze their function and survival in vivo. Here we provide

surprising evidence that RAG expression in uncommitted hematopoietic progenitors and NK cell precursors marks functionally distinct subsets of NK cells in the periphery, demonstrating both a novel role for RAG in the functional specialization of the NK cell lineage and a physiological role for RAG proteins outside of V(D)J recombination.

Although the mechanism behind stochastic expression of RAG in developing NK cells (only half in bone marrow show evidence of previously expressing RAG) is not known, mutant NK cells lacking RAG (or RAG activity) or WT NK cells lacking a history of RAG expression are more terminally differentiated and highly cytolytic, but these short-lived effector cells are characterized by greater apoptosis and γ-H2AX staining at steady state and by an inability to remove the γ-H2AX foci following DNA damage. In contrast, WT NK cells with a history of RAG expression are less terminally differentiated and cytotoxic but can generate long-lived memory cells following antigen-specific proliferation, characterized by increased survival and ability to repair DNA DSBs. Therefore, there exists an unexpected functional dichotomy between NK cell populations in which RAG expression and, likely, RAG-generated DNA breaks are used for the purpose of creating a long-lived NK cell pool to combat pathogens. It remains to be determined whether this represents an evolutionary mechanism that is tolerated despite risks of genomic instability or whether it represents a risk-free utilization of RAG endonuclease activity outside of V(D)J recombination. RAG is capable of generating single-strand nicks and DSBs in DNA, and either or both could be contributing to NK cell fitness. We cannot predict the putative sites at which such damage is inflicted because little is known regarding the targeting of RAG1 (the subunit with endonuclease activity) outside of antigen receptor loci (Ji et al., 2010). Further transcriptome analysis will be required to determine whether NK cells that have previously expressed RAG become functionally specialized through upregulation of lymphoid-related transcription factors, resulting in the cellular "fitness" observed following periods of robust proliferation and cellular stress.

Interestingly, a parallel heterogeneity has been ascribed to peripheral CD8+ T cells following an antigen encounter. In the context of pathogen infection, responding CD8+ T cells are currently thought to generate a heterogeneous effector population consisting of KLRG1hi short-lived effector cells (SLECs) that are more terminally differentiated and KLRG1lo memory precursor effector cells (MPECs) that can give rise to long-lived memory cells (Kaech and Wherry, 2007). Given that NK cells are similar in function and phenotype to effector/memory CD8+ T cells (Sun and Lanier, 2011), it will be of interest to determine whether SLECs also possess decreased genomic stability and DNA damage repair capability compared with MPECs.

Heterogeneity within the NK cell compartment, as defined by prior RAG expression, may also exist in humans. Humans lacking RAG activity exhibit severe combined immunodeficiency (Schwarz et al., 1996) with the absence of T and B cells but possessing NK cells, whereas partial loss of RAG activity results in Omenn syndrome (Villa et al., 1998) or combined immunodeficiency. Some of these RAG mutant patients have been reported to be sensitive to radiation, presumably because of an inability to efficiently repair therapy-induced DNA DSBs (Blunt et al., 1996; Nicolas et al., 1998; Villa et al., 1998). Similarly, SCID and RAG-

deficient mice are more sensitive to full body irradiation than WT mice (Biedermann et al., 1991), and it will be of interest to determine whether the greater morbidity and mortality of irradiated RAG-deficient mice is related to greater genomic instability. Given that NK cells from SCID mice behaved like the RAG-deficient cells, we predict that mice deficient in ATM or Ku80 would similarly exhibit defects in the NK cell response to viral infection because of loss of gross genome integrity from the accumulation of unrepaired DNA DSBs. In addition, because SCID NK cells exhibited an activated phenotype and enhanced cytotoxicity like RAG-deficient NK cells, it is possible that DNA-PKcs is important for signaling downstream of RAG-mediated breaks early during NK cell ontogeny. Interestingly, the spectrum of RAG-related disorders often manifests in humans with autoimmunity and human cytomegalovirus (HCMV) infection (de Villartay et al., 2005). Because virus-specific effector and memory NK cell responses to HCMV infection have been documented recently (Björkström et al., 2011; Della Chiesa et al., 2012; Foley et al., 2012; Lopez-Vergès et al., 2011), it will be of interest to determine whether lack of HCMV control in individuals with SCID or Omenn syndrome is due to a decreased cellular fitness in NK cells responding to infection.

Although our findings suggest that selective RAG expression in developing lymphocytes confers resistance to DNA damage, the molecular mechanisms behind this preservation of cellular fitness at steady state and during cellular stress remain unclear. Because the Rag1−/− D708A NK cells (possessing a RAG1 catalytic mutant) show a similar defect as Rag1−/− NK cells during MCMV infection, we infer that RAG-mediated cleavage events during NK cell ontogeny are essential for initiating the induction of DNA repair enzymes, thereby educating the developing NK cell to better respond to subsequent DNA damage as a peripheral mature lymphocyte. The prediction that a "feed forward" mechanism exists in developing lymphocytes whereby intentional DNA breaks and recruitment of DNA damage response proteins result in a replenishing or even enhancement of additional damage response proteins remains to be tested further. A close correlation has been reported between RAG2 binding and the activating H3K4me3 histone mark at the promoters of many tissue-specific genes throughout the genome (Ji et al., 2010; Liu et al., 2007; Matthews et al., 2007), and epigenetic analysis of regulatory regions surrounding DNA damage repair genes in WT compared with RAG-deficient NK cells may provide mechanistic insights into how damage response protein levels are set in an individual resting lymphocyte. It is possible that the RAG1/2 complex plays a regulatory function during ontogeny at sites lacking RSS sequences, resulting in changes in transcriptional activity, histone modifications, or chromatin structure of non-antigen receptor loci.

Although we have demonstrated that RAG deficiency results in a reduced cellular fitness in NK cells that is revealed during the response against viral infection, this novel role for RAG is not restricted to NK cells. Interestingly, the decrease in DNA-PKcs, Ku80, and ATM transcripts and the aberrant upregulation and clearance of the γ-H2AX mark observed in NK cells from Rag2−/− mice were also observed in OT-1 CD8+ T cells on a Rag2−/− background compared with WT OT-1 cells. Although OT-1 x Rag2−/− cells did not persist as well as WT OT-1 cells

following viral challenge, this survival defect was not as pronounced as with $Rag2^{-/-}$ versus WT NK cells, suggesting that T cells possess additional mechanisms conferring longevity relative to NK cells. These data, along with our observation of differential RAG expression and γ-H2AX levels within ILC subsets, raise the possibility that RAG activity modulates cellular fitness in B cells as well as in other "innate" lymphocyte populations (e.g., NKT cells, γδ T cells, B1 B cells, and even dendritic cells of lymphoid origin).

Additional studies will investigate how stochastic RAG expression induces the DNA damage response proteins in lymphocytes during ontogeny and determines both the "set point" for DNA DSB repair enzymes in resting lymphocytes and the ability of activated and proliferating lymphocytes to repair DSBs. Irrespective of the precise molecular mechanism behind the RAG-endowed cellular fitness of lymphocytes, it is fascinating to envision a paradigm where a programmed DNA endonuclease like RAG is able to stably "imprint" the functional properties of a developmental lineage long after it has acted on it. Our findings identify a novel role for the RAG proteins and add to a growing body of evidence implicating "controlled" DNA damage in the regulation of gene expression, cell development, and cell fate in eukaryotes (Abramson et al., 2010; Bredemeyer et al., 2008; Ju et al., 2006; Larsen and Megeney, 2010; Larsen et al., 2010; Schroeder et al., 2013).

EXPERIMENTAL PROCEDURES

Mice

C57BL/6, B6.SJL (CD45.1), $Ly49h^{-/-}$, $Rag2^{-/-}$, $Rag1^{-/-}$, SCID, nude, OT-1, OT-1x$Rag2^{-/-}$, $Rag2^{-/-}xIl2rg^{-/-}$, and $B2m^{-/-}$ mice were maintained at Memorial Sloan Kettering Cancer Center, whereas $Rag1^{-/-}$ D708A mice were maintained at Yale School of Medicine. $Rag1^{cre}$ x $ROSA26^{tdRFP}$ and $Rag2^{YFP}$ mice were provided by P. Kincade (University of Oklahoma) and P. Fink (University of Washington), respectively. Mixed bone marrow chimeric mice were generated as described previously (Sun et al., 2009). All animals were generated and maintained in accordance with the guidelines of the Memorial Sloan Kettering Cancer Center Institutional Animal Care and Use Committee.

Virus Infections

MCMV (Smith strain) and MCMV-Ova were passaged serially through BALB/c mice two to three times, and viral stocks were prepared from salivary glands. Mice were infected with 7.5×10^3 plaque-forming units (pfu) MCMV by intraperitoneal (i.p.) injection. For the adoptive transfer studies, recipient $Ly49h^{-/-}$ mice were infected with 7.5×10^2 pfu MCMV by i.p. injection 1 day after receiving approximately 5×10^5 Ly49H+ NK cells.

Flow Cytometry and Cell Sorting

Single-cell suspensions were generated from the indicated organs and stained with the indicated fluorophore-conjugated antibodies (BD Biosciences, eBioscience, BioLegend, and Tonbo). For staining of OT-1 cells, MHC class I tetramers were generated by conjugating K^b/SIINFEKL monomers (NIH Tetramer Facility) to streptavidin-phycoerythrin (BD Biosciences). For staining nuclear proteins and γ-H2AX (Millipore), cells were fixed and permeabilized with the transcription factor staining kit (eBioscience and Tonbo). Pan-caspase staining was carried out using the carboxyfluorescein FLICA in vitro poly caspase kit (Immunochemistry Technologies). As a positive control, cells were first incubated with 20 μg/ml of α-mouse CD95 (clone Jo-2, BD Pharmingen) for 2.5–4 hr at 37°C (data not shown). Flow cytometry and cell sorting were performed on the LSR II and Aria II cytometers (BD Biosciences), respectively. Data were analyzed with FlowJo software (Tree Star).

Ex Vivo T Cell Stimulation

Equal numbers of OT-1 (CD45.1) and OT-1 x $Rag2^{-/-}$ (CD45.2) T cells were cocultured in complete RPMI + 10% fetal bovine serum with 1:1,000 2-mercaptoethanol (Sigma) containing 1 μM SIINFEKL peptide or anti-CD3/28 beads (Life Technologies).

BrdU Treatment and Staining

Mice were given BrdU (Sigma) (0.8 mg/ml) in drinking water for 2 weeks ("pulse") and then given normal drinking water ("chase"). After various periods of time on normal drinking water, isolated lymphocytes from labeled mice were first stained for expression of surface markers, and, after fixation, the cells were then stained with an anti-BrdU monoclonal antibody (BD Biosciences).

NK Cell Enrichment and Adoptive Transfer

NK cells were enriched by removing T, B, and red blood cells from total splenocyte suspensions using rat IgG against mouse CD4, CD8, CD19, and Ter119 (University of California at San Francisco Core Facility, 10 μg of each antibody per spleen), followed by anti-rat IgG-coupled magnetic beads (QIAGEN) and magnetic depletion. Approximately 5×10^5 enriched NK cells were injected intravenously into adult recipient mice 1 day before MCMV infection. In some experiments, NK cells or unfractionated splenocytes were labeled with varying concentrations of CFSE before intravenous injection. Labeling of cells with CFSE was performed in accordance with the manufacturer's instructions (Invitrogen).

Ex Vivo and In Vivo Cytotoxicity Assays

Enriched NK cells were used as effector cells ex vivo in a 6 hr ^{51}Cr release assay against m157-transfected Ba/F3 and Yac1 target cells. The percentage of total and Ly49H+ NK cells in each group was determined by flow cytometry, and absolute numbers were normalized before incubation with targets. Large numbers of NK cells from Ly49H-deficient mice and use of untransduced Ba/F3 as target cells were included as negative controls to demonstrate the specificity of receptor-ligand interactions (data not shown).

The in vivo cytotoxicity of NK cells was investigated by labeling WT and $B2m^{-/-}$ splenocytes with different amounts of CFSE (Invitrogen) and transferring a 1:1 WT:$B2m^{-/-}$ mixture into $Rag2^{-/-}$ or WT recipient mice. Percent lysis of transferred cells was determined at various time points.

Quantitative RT-PCR

Sorted NK cells were lysed in Tri-Reagent (Ambion). RNA purification and cDNA synthesis were carried out with the QIAGEN RNeasy kit (with DNase I treatment), and MulV reverse transcriptase and Oligo dT(116) primers (Applied Biosystems). iQ Sybr Green SuperMix (Bio-Rad) was used for quantitative RT-PCR (qRT-PCR). Data were normalized to β-actin and expressed as relative target abundance via the ΔΔCT method. Table S1 lists the relevant primer sequences.

Isolation of ILC Subsets

Mesenteric lymph nodes and Peyer patches were extracted and mechanically crushed into single-cell suspensions. Lungs, intestines, and fat were digested in collagenase type 4 (Worthington Biochemical), collagenase D (Roche), and collagenase type 2 (Worthington Biochem), respectively.

Statistical Analysis

Data were analyzed on GraphPad Prism using one-way ANOVA and unpaired Student's t test, and differences were considered significant at p values of less than 0.05.

SUPPLEMENTAL INFORMATION

Supplemental Information includes Extended Experimental Procedures, seven figures, and one table and can be found with this article online at http://dx.doi.org/10.1016/j.cell.2014.08.026.

REFERENCES

Abramson, J., Giraud, M., Benoist, C., and Mathis, D. (2010). Aire's partners in the molecular control of immunological tolerance. Cell 140, 123–135.

Agrawal, A., and Schatz, D.G. (1997). RAG1 and RAG2 form a stable post-cleavage synaptic complex with DNA containing signal ends in V(D)J recombination. Cell 89, 43–53.

Andrews, D.M., and Smyth, M.J. (2010). A potential role for RAG-1 in NK cell development revealed by analysis of NK cells during ontogeny. Immunol. Cell Biol. 88, 107–116.

Biedermann, K.A., Sun, J.R., Giaccia, A.J., Tosto, L.M., and Brown, J.M. (1991). scid mutation in mice confers hypersensitivity to ionizing radiation and a deficiency in DNA double-strand break repair. Proc. Natl. Acad. Sci. USA 88, 1394–1397.

Björkström, N.K., Lindgren, T., Stoltz, M., Fauriat, C., Braun, M., Evander, M., Michaëlsson, J., Malmberg, K.J., Klingström, J., Ahlm, C., and Ljunggren, H.G. (2011). Rapid expansion and long-term persistence of elevated NK cell numbers in humans infected with hantavirus. J. Exp. Med. 208, 13–21.

Blunt, T., Gell, D., Fox, M., Taccioli, G.E., Lehmann, A.R., Jackson, S.P., and Jeggo, P.A. (1996). Identification of a nonsense mutation in the carboxyl-terminal region of DNA-dependent protein kinase catalytic subunit in the scid mouse. Proc. Natl. Acad. Sci. USA 93, 10285–10290.

Borghesi, L., Hsu, L.Y., Miller, J.P., Anderson, M., Herzenberg, L., Herzenberg, L., Schlissel, M.S., Allman, D., and Gerstein, R.M. (2004). B lineage-specific regulation of V(D)J recombinase activity is established in common lymphoid progenitors. J. Exp. Med. 199, 491–502.

Bosma, G.C., Custer, R.P., and Bosma, M.J. (1983). A severe combined immunodeficiency mutation in the mouse. Nature 301, 527–530.

Bredemeyer, A.L., Sharma, G.G., Huang, C.Y., Helmink, B.A., Walker, L.M., Khor, K.C., Nuskey, B., Sullivan, K.E., Pandita, T.K., Bassing, C.H., and Sleckman, B.P. (2006). ATM stabilizes DNA double-strand-break complexes during V(D)J recombination. Nature 442, 466–470.

Bredemeyer, A.L., Helmink, B.A., Innes, C.L., Calderon, B., McGinnis, L.M., Mahowald, G.K., Gapud, E.J., Walker, L.M., Collins, J.B., Weaver, B.K., et al. (2008). DNA double-strand breaks activate a multi-functional genetic program in developing lymphocytes. Nature 456, 819–823.

Chen, H.T., Bhandoola, A., Difilippantonio, M.J., Zhu, J., Brown, M.J., Tai, X., Rogakou, E.P., Brotz, T.M., Bonner, W.M., Ried, T., and Nussenzweig, A. (2000). Response to RAG-mediated VDJ cleavage by NBS1 and gamma-H2AX. Science 290, 1962–1965.

de Villartay, J.P., Lim, A., Al-Mousa, H., Dupont, S., Déchanet-Merville, J., Coumau-Gatbois, E., Gougeon, M.L., Lemainque, A., Eidenschenk, C., Jouanguy, E., et al. (2005). A novel immunodeficiency associated with hypomorphic RAG1 mutations and CMV infection. J. Clin. Invest. 115, 3291–3299.

Della Chiesa, M., Falco, M., Podestà, M., Locatelli, F., Moretta, L., Frassoni, F., and Moretta, A. (2012). Phenotypic and functional heterogeneity of human NK cells developing after umbilical cord blood transplantation: a role for human cytomegalovirus? Blood 119, 399–410.

Fernandez-Capetillo, O., Lee, A., Nussenzweig, M., and Nussenzweig, A. (2004). H2AX: the histone guardian of the genome. DNA Repair (Amst.) 3, 959–967.

Foley, B., Cooley, S., Verneris, M.R., Pitt, M., Curtsinger, J., Luo, X., Lopez-Vergès, S., Lanier, L.L., Weisdorf, D., and Miller, J.S. (2012). Cytomegalovirus reactivation after allogeneic transplantation promotes a lasting increase in educated NKG2C+ natural killer cells with potent function. Blood 119, 2665–2674.

Fronková, E., Krejcí, O., Kalina, T., Horváth, O., Trka, J., and Hrusák, O. (2005). Lymphoid differentiation pathways can be traced by TCR delta rearrangements. J. Immunol. 175, 2495–2500.

Fugmann, S.D., Lee, A.I., Shockett, P.E., Villey, I.J., and Schatz, D.G. (2000a). The RAG proteins and V(D)J recombination: complexes, ends, and transposition. Annu. Rev. Immunol. 18, 495–527.

Fugmann, S.D., Villey, I.J., Ptaszek, L.M., and Schatz, D.G. (2000b). Identification of two catalytic residues in RAG1 that define a single active site within the RAG1/RAG2 protein complex. Mol. Cell 5, 97–107.

Fulop, G.M., and Phillips, R.A. (1990). The scid mutation in mice causes a general defect in DNA repair. Nature 347, 479–482.

Gellert, M. (2002). V(D)J recombination: RAG proteins, repair factors, and regulation. Annu. Rev. Biochem. 71, 101–132.

Gostissa, M., Alt, F.W., and Chiarle, R. (2011). Mechanisms that promote and suppress chromosomal translocations in lymphocytes. Annu. Rev. Immunol. 29, 319–350.

Helmink, B.A., and Sleckman, B.P. (2012). The response to and repair of RAG-mediated DNA double-strand breaks. Annu. Rev. Immunol. 30, 175–202.

Hiom, K., and Gellert, M. (1998). Assembly of a 12/23 paired signal complex: a critical control point in V(D)J recombination. Mol. Cell 1, 1011–1019.

Hogquist, K.A., Jameson, S.C., Heath, W.R., Howard, J.L., Bevan, M.J., and Carbone, F.R. (1994). T cell receptor antagonist peptides induce positive selection. Cell 76, 17–27.

Ichii, M., Shimazu, T., Welner, R.S., Garrett, K.P., Zhang, Q., Esplin, B.L., and Kincade, P.W. (2010). Functional diversity of stem and progenitor cells with B-lymphopoietic potential. Immunol. Rev. 237, 10–21.

Igarashi, H., Kuwata, N., Kiyota, K., Sumita, K., Suda, T., Ono, S., Bauer, S.R., and Sakaguchi, N. (2001). Localization of recombination activating gene 1/green fluorescent protein (RAG1/GFP) expression in secondary lymphoid organs after immunization with T-dependent antigens in rag1/gfp knockin mice. Blood 97, 2680–2687.

Ji, Y., Resch, W., Corbett, E., Yamane, A., Casellas, R., and Schatz, D.G. (2010). The in vivo pattern of binding of RAG1 and RAG2 to antigen receptor loci. Cell 141, 419–431.

Ju, B.G., Lunyak, V.V., Perissi, V., Garcia-Bassets, I., Rose, D.W., Glass, C.K., and Rosenfeld, M.G. (2006). A topoisomerase IIbeta-mediated dsDNA break required for regulated transcription. Science 312, 1798–1802.

Kaech, S.M., and Wherry, E.J. (2007). Heterogeneity and cell-fate decisions in effector and memory CD8+ T cell differentiation during viral infection. Immunity 27, 393–405.

Kim, D.R., Dai, Y., Mundy, C.L., Yang, W., and Oettinger, M.A. (1999). Mutations of acidic residues in RAG1 define the active site of the V(D)J recombinase. Genes Dev. 13, 3070–3080.

Kondo, M., Weissman, I.L., and Akashi, K. (1997). Identification of clonogenic common lymphoid progenitors in mouse bone marrow. Cell 91, 661–672.

Kuwata, N., Igarashi, H., Ohmura, T., Aizawa, S., and Sakaguchi, N. (1999). Cutting edge: absence of expression of RAG1 in peritoneal B-1 cells detected by knocking into RAG1 locus with green fluorescent protein gene. J. Immunol. 163, 6355–6359.

Landree, M.A., Wibbenmeyer, J.A., and Roth, D.B. (1999). Mutational analysis of RAG1 and RAG2 identifies three catalytic amino acids in RAG1 critical for both cleavage steps of V(D)J recombination. Genes Dev. 13, 3059–3069.

Lanier, L.L., Chang, C., Spits, H., and Phillips, J.H. (1992). Expression of cytoplasmic CD3 epsilon proteins in activated human adult natural killer (NK) cells

and CD3 gamma, delta, epsilon complexes in fetal NK cells. Implications for the relationship of NK and T lymphocytes. J. Immunol. *149*, 1876–1880.

Larsen, B.D., and Megeney, L.A. (2010). Parole terms for a killer: directing caspase3/CAD induced DNA strand breaks to coordinate changes in gene expression. Cell Cycle *9*, 2940–2945.

Larsen, B.D., Rampalli, S., Burns, L.E., Brunette, S., Dilworth, F.J., and Megeney, L.A. (2010). Caspase 3/caspase-activated DNase promote cell differentiation by inducing DNA strand breaks. Proc. Natl. Acad. Sci. USA *107*, 4230–4235.

Lee, G.S., Neiditch, M.B., Salus, S.S., and Roth, D.B. (2004). RAG proteins shepherd double-strand breaks to a specific pathway, suppressing error-prone repair, but RAG nicking initiates homologous recombination. Cell *117*, 171–184.

Lieber, M.R., Yu, K., and Raghavan, S.C. (2006). Roles of nonhomologous DNA end joining, V(D)J recombination, and class switch recombination in chromosomal translocations. DNA Repair (Amst.) *5*, 1234–1245.

Liu, Y., Subrahmanyam, R., Chakraborty, T., Sen, R., and Desiderio, S. (2007). A plant homeodomain in RAG-2 that binds Hypermethylated lysine 4 of histone H3 is necessary for efficient antigen-receptor-gene rearrangement. Immunity *27*, 561–571.

Lopez-Vergès, S., Milush, J.M., Schwartz, B.S., Pando, M.J., Jarjoura, J., York, V.A., Houchins, J.P., Miller, S., Kang, S.M., Norris, P.J., et al. (2011). Expansion of a unique CD57+NKG2Chi natural killer cell subset during acute human cytomegalovirus infection. Proc. Natl. Acad. Sci. USA *108*, 14725–14732.

Matthews, A.G., Kuo, A.J., Ramón-Maiques, S., Han, S., Champagne, K.S., Ivanov, D., Gallardo, M., Carney, D., Cheung, P., Ciccone, D.N., et al. (2007). RAG2 PHD finger couples histone H3 lysine 4 trimethylation with V(D)J recombination. Nature *450*, 1106–1110.

Mills, K.D., Ferguson, D.O., and Alt, F.W. (2003). The role of DNA breaks in genomic instability and tumorigenesis. Immunol. Rev. *194*, 77–95.

Mombaerts, P., Iacomini, J., Johnson, R.S., Herrup, K., Tonegawa, S., and Papaioannou, V.E. (1992). RAG-1-deficient mice have no mature B and T lymphocytes. Cell *68*, 869–877.

Nicolas, N., Moshous, D., Cavazzana-Calvo, M., Papadopoulo, D., de Chasseval, R., Le Deist, F., Fischer, A., and de Villartay, J.P. (1998). A human severe combined immunodeficiency (SCID) condition with increased sensitivity to ionizing radiations and impaired V(D)J rearrangements defines a new DNA recombination/repair deficiency. J. Exp. Med. *188*, 627–634.

Nussenzweig, A., and Nussenzweig, M.C. (2010). Origin of chromosomal translocations in lymphoid cancer. Cell *141*, 27–38.

Oettinger, M.A., Schatz, D.G., Gorka, C., and Baltimore, D. (1990). RAG-1 and RAG-2, adjacent genes that synergistically activate V(D)J recombination. Science *248*, 1517–1523.

Papaemmanuil, E., Rapado, I., Li, Y., Potter, N.E., Wedge, D.C., Tubio, J., Alexandrov, L.B., Van Loo, P., Cooke, S.L., Marshall, J., et al. (2014). RAG-mediated recombination is the predominant driver of oncogenic rearrangement in ETV6-RUNX1 acute lymphoblastic leukemia. Nat. Genet. *46*, 116–125.

Pilbeam, K., Basse, P., Brossay, L., Vujanovic, N., Gerstein, R., Vallejo, A.N., and Borghesi, L. (2008). The ontogeny and fate of NK cells marked by permanent DNA rearrangements. J. Immunol. *180*, 1432–1441.

Rogakou, E.P., Pilch, D.R., Orr, A.H., Ivanova, V.S., and Bonner, W.M. (1998). DNA double-stranded breaks induce histone H2AX phosphorylation on serine 139. J. Biol. Chem. *273*, 5858–5868.

Rogakou, E.P., Nieves-Neira, W., Boon, C., Pommier, Y., and Bonner, W.M. (2000). Initiation of DNA fragmentation during apoptosis induces phosphorylation of H2AX histone at serine 139. J. Biol. Chem. *275*, 9390–9395.

Schroeder, E.A., Raimundo, N., and Shadel, G.S. (2013). Epigenetic silencing mediates mitochondria stress-induced longevity. Cell Metab. *17*, 954–964.

Schwarz, K., Gauss, G.H., Ludwig, L., Pannicke, U., Li, Z., Lindner, D., Friedrich, W., Seger, R.A., Hansen-Hagge, T.E., Desiderio, S., et al. (1996). RAG mutations in human B cell-negative SCID. Science *274*, 97–99.

Shinkai, Y., Rathbun, G., Lam, K.P., Oltz, E.M., Stewart, V., Mendelsohn, M., Charron, J., Datta, M., Young, F., Stall, A.M., et al. (1992). RAG-2-deficient mice lack mature lymphocytes owing to inability to initiate V(D)J rearrangement. Cell *68*, 855–867.

Spits, H., and Cupedo, T. (2012). Innate lymphoid cells: emerging insights in development, lineage relationships, and function. Annu. Rev. Immunol. *30*, 647–675.

Sun, J.C., and Lanier, L.L. (2011). NK cell development, homeostasis and function: parallels with CD8+ T cells. Nat. Rev. Immunol. *11*, 645–657.

Sun, J.C., Beilke, J.N., and Lanier, L.L. (2009). Adaptive immune features of natural killer cells. Nature *457*, 557–561.

Villa, A., Santagata, S., Bozzi, F., Giliani, S., Frattini, A., Imberti, L., Gatta, L.B., Ochs, H.D., Schwarz, K., Notarangelo, L.D., et al. (1998). Partial V(D)J recombination activity leads to Omenn syndrome. Cell *93*, 885–896.

Welner, R.S., Esplin, B.L., Garrett, K.P., Pelayo, R., Luche, H., Fehling, H.J., and Kincade, P.W. (2009). Asynchronous RAG-1 expression during B lymphopoiesis. J. Immunol. *183*, 7768–7777.

Yang, Q., Saenz, S.A., Zlotoff, D.A., Artis, D., and Bhandoola, A. (2011). Cutting edge: Natural helper cells derive from lymphoid progenitors. J. Immunol. *187*, 5505–5509.